Research Article

BIOMEDICAL Journal of Scientific & Technical Research

ISSN: 2574 -1241

DOI: 10.26717/BJSTR.2024.55.008740

Susceptibility MRI in Brain Nuclei Improves Early Diagnosis of Parkinson's Disease Using Linear Discriminant Analysis Method

Jian Zhang Xia[1], Ya Bin Jin[2], Yun Jie Rong[3], Wen Xiu Wu[4], Ming Yong Gao[4], Hai Mei Huang[1,4] and Zhi Feng Xu[4]*

[1]*Department of Radiology, Fifth People's Hospital of NanHai District, China*

[2]*Department of Clinical Research Institute, First People's Hospital of Foshan, China*

[3]*Department of Radiology, Second Affiliated Hospital of Shantou University Medical College, China*

[4]*Department of Radiology, First People's Hospital of Foshan, China*

***Corresponding author:** Zhi Feng Xu, Department of Radiology, The First People's Hospital of Foshan, 81 Lingnan Avenue, Guagndong, 528000, China

ARTICLE INFO

Received: March 14, 2024

Published: March 21, 2024

Citation: Jian Zhang Xia, Ya Bin Jin, Yun Jie Rong, Wen Xiu Wu, Ming Yong Gao, Hai Mei Huang and Zhi Feng Xu. Susceptibility MRI in Brain Nuclei Improves Early Diagnosis of Parkinson's Disease Using Linear Discriminant Analysis Method. Biomed J Sci & Tech Res 55(4)-2024. BJSTR. MS.ID.008740.

ABSTRACT

The study aimed to explore a new imaging biomarker based on quantitative susceptibility mapping (QSM) using linear discriminant analysis (LDA) method for improving early diagnosis of Parkinson's disease. 34 PD patients and 15 controls were enrolled, and the PD patients were divided into two groups (early-stage and advanced-stage groups) based on the Hoehn-Yahr assessment. Magnetic susceptibilities in six brain structures, including the caudate nucleus (CN), globus pallidus (GP), thalamus (THA), putamen (PUT), substantia nigra (SN) and red nucleus (RN), were measured. Mean susceptibilities were measured and compared between the PD patients and controls. Linear discriminant analysis (LDA) of machine learning (ML) was applied to integrate the magnetic susceptibilities in all nuclei as a new biomarker (LDA biomarker). ROC curves were calculated to evaluate the effectiveness of various indicators. Susceptibilities in all nuclei showed an increase in heterogeneity in the PD patients. Compared to the controls, the PD patients had significantly increased magnetic susceptibilities in the PUT and THA, and there were significant differences in the THA between the controls and early-PD patients. The LDA biomarker had the highest AUC (0.784) for classifying PD patients and making an early PD diagnosis (0.777). LDA biomarker derived from ML based on QSM is a promising tool for early diagnosis and advanced assessment of PD.

Keywords: Parkinson's Disease; Machine Learning; Iron Deposition; Quantitative Susceptibility Mapping; Linear Discriminant Analysis

Abbreviations: QSM: Quantitative Susceptibility Mapping; LDA: Linear Discriminant Analysis; CN: Caudate Nucleus; GP: Globus Pallidus; SN: Substantia Nigra; RN: Red Nucleus; LDA: Linear Discriminant Analysis; ML: Machine Learning

Introduction

The diagnosis of Parkinson's disease (PD) in clinical practice lacks objective verification and mainly based on motor symptoms, which have not yielded great accuracy [1,2]. Significant motor symptoms generally emerge in the advanced stage resulted in poor prognosis and poor quality of life. Nevertheless, the accuracy of early diagnosis is only approximately 50% according to routine clinical practice [2], indicating an urgent need for a reliable biological marker to confirm PD diagnosis and monitor its progression. To meet the above requirements, potential biomarker should be related to the mechanisms and pathophysiology of PD. Cerebral iron plays an important role as the synthesis of neurotransmitters. In contrast, iron overload in the brain would promote apoptosis of dopamine (DA) neurons [3,4] due to iron-related oxidative reactions and neurotoxicity. In vivo and autopsy studies have provided evidence of iron overload in the substantia nigra (SN) of PD patients [2,5,6] Quantitative and distri-

bution characteristics of brain iron is a promising biomarker for PD diagnosis and for progression monitoring [5,6]. It may be helpful for making a clinical diagnosis of PD. Advanced MR imaging techniques were used for brain iron imaging in PD, such as susceptibility contrasts (T2*-weighted imaging and R2* [1/T2*] mapping), relaxation contrast (T2-weighted imaging), quantitative susceptibility mapping (QSM) and susceptibility weighted imaging (SWI), provided objective measures of the magnetic susceptibility value of iron quantitatively in the deep brain nuclei [6-8]. QSM has been proposed to be a powerful tool for the quantitative analysis of brain iron because it is more accurate than transverse relaxation rates for iron quantification [5,8,9]. QSM has shown more sensitivity over R2* mapping in multiple sclerosis patients evaluation based on regional iron accumulation [10].

Progressive regional iron deposition, including its levels and spatial distribution, has been found in the deep gray nuclei, including the caudate nucleus (CN), globus pallidus (GP), thalamus (THA), putamen (PUT), substantia nigra (SN) and red nucleus (RN), and especially in the SN, PUT and GP, which are the main regions impaired in PD. Compared to controls, most but not all studies have suggested that iron accumulation increased significantly in all these nuclei in PD patients [7,11-13]. However, these results have not been replicated between studies. In addition, differences at the level of nuclei measurement is also an important reason for these inconsistent results. Each nuclear cluster was previously studied as a separate area, in fact, the functions of these nuclei do not occur in isolation, and these tasks are carried out through the internal connections between each nuclei and compensatory mechanisms [13-15]. The mean value of magnetic susceptibilities of all deep nuclei was used to distinguish PD patients and healthy controls [16,17]. Previous studies have demonstrated that the voxel-wise magnetic susceptibility of the whole brain,13 diagnostic performance of QSM combined with histogram analysis and multivariate logistic regression analysis in mutiple nuclei [18], and machine learning models derived from Random Forest (RF), Extreme Gradient Boosting (XGB), and Light Gradient Boosting (LGB) and trained with the mean QSM-based magnetic susceptibilities extracted from multiple brain regions [14] could improve the identification and discrimination ability of PD.Linear discriminant analysis (LDA) is a supervised dimension reduction method to measure the difference of labels and categories. Compared with the ambiguity of principal component analysis (PCA), LDA has a clearer purpose and can better reflect the differences between samples [19].

At the same time, the corresponding weight factors are given to different features. Several studies have revealed the advantage of the diagnostic capabilities of clinical features such as voice signal [20], blood biomarkers [21] and MRI data [22] combined with LDA to distinguish PD patients from healthy controls, assess disease progression and distinguish it from other degenerative diseases. We hypothesize that the clear deposition characteristics and accurate quantification of iron in multiple deep brain nuclei would be helpful to improve early diagnosis and advanced assessment of PD. Therefore, to test this hypothesis, the diagnostic performance of the LDA classifier to identify PD was compared to those of several single nuclei.

Materials and Methods

Subjects

The study comprised 34 PD patients and 15 controls in our institution between March 2019 and December 2019. PD was diagnosed according to the MDS clinical diagnostic criteria (2015). In addition, PD patients were divided into two subgroups based on Hoehn-Yahr stages (clinical disease stage), namely, the early-stage (H&Y1-2) and advanced-stage (H&Y3-5) groups. The control group had no history of neurological or psychiatric disorders. Indications for their examination included headache, cerebral artery aneurysms, benign positional vertigo, hemifacial spasm and bilateral upper extremity numbness. In all subjects, conventional MR imaging (T1- and T2-weighted imaging, T2w-FLAIR and diffusion-weighted imaging) results were normal. All subjects were free of major acute and chronic medical issues such as liver, kidney or thyroid abnormalities, diabetes, stroke and severe hypertension. Patients with other known neurodegenerative disorders or with microbleeds or vascular dysmorphia in the deep brain nuclei were excluded. The main characteristics of the study participants are summarized in (Table 1). Our study was approved by the institutional review board of First People's Hospital of Foshan (ID: L(2018).4th). Informed consent was obtained from all participants.

Table 1: Clinical and demographic data of the study cohort.

	Controls	Parkinson's disease (PD)			p value			
		Summary	Early stage (H&Y 1-2)	Progressive stage (H&Y 3-5)	Control vs. PD	Control vs. early stage	Control vs. progressive stage	Early stage vs. progressive stage
N	15	34	20	14	NA	NA	NA	NA
N, male (%)	5(33.3%)	15(44.1%)	9(45.0%)	6(42.9%)	0.479	0.486	0.597	0.901
Age (years)†	64.4 (8.8)	64.6 (9.7)	64.1(9.1)	65.5 (10.7)	0.933	0.915	0.757	0.664
Disease duration (months)††	NA	52.7(1-240)	25.2(1-60)	92.0(24-240)	NA	NA	NA	0.000

Note: † mean(standard deviation)

†† = median (range)

MR Image Acquisition

All examinations were performed on a 3.0-T MR system (Discovery MR 750; GE Healthcare) equipped with an eight-channel head coil. To avoid moving artifacts, the head was fixed with the sponges. Traditional MRI sequences[T2-weighted imaging (T2w), T1-weighted imaging (T1w), and fluid-attenuated inversion recovery (FLAIR)] were performed with the following parameters: T2w (TR: 2500 ms, TE: 60 ms), T1w (TR: 450 ms, TE: 3.5 ms) and T2-FLAIR (TR: 8500 ms, TE: 128 ms). All sequences take the following parameter, such as thickness 4 mm, space 1.5 mm, matrix 320×192, and field of view (FOV) 24cm×24cm. QSM was obtained with a 3D flow-compensated multiecho spoiled gradient echo sequence. The parameters were as follows: TR: 58 ms; TE1: 4.5 ms; TE spacing: 5 ms; number of TEs: 11; flip angle: 15°; bandwidth, 62.5 Hz; matrix: 256×512; thickness: 2 mm; FOV: 22cm×22cm. All images were visually inspected to ensure that no visible artifacts were included in the subsequent analyses.

QSM Data Analysis

QSM raw data were processed by using QSM analysis software (AW4.7, GE America), as conducted in previous studies [9,11,12] and MEDI Toolbox (http://pre.weill.cornell.edu/mri/pages/qsm.html). Six regions of interest (ROIs) within the deep nuclei system (including the CN, GP, PUT, THA, SN and RN) were drawn manually on the QSM maps (Figure 1). Data of each region was obtained from the largest cross section clearly discernible to the naked eye. The magnetic susceptibility of each ROI was calculated from the average of both sides. In order to more accurately depict the ROIs, the QSM images were magnified 3-4 times, and the ROIs were marked and confirmed by two neuroradiologists with 10 years of experience in neuroimaging and were blinded to the subject data. For each subject (patients with PD and controls), the mean magnetic susceptibilities obtained by the two neuroradiologists as the final values, and all statistical analyses used those final values.

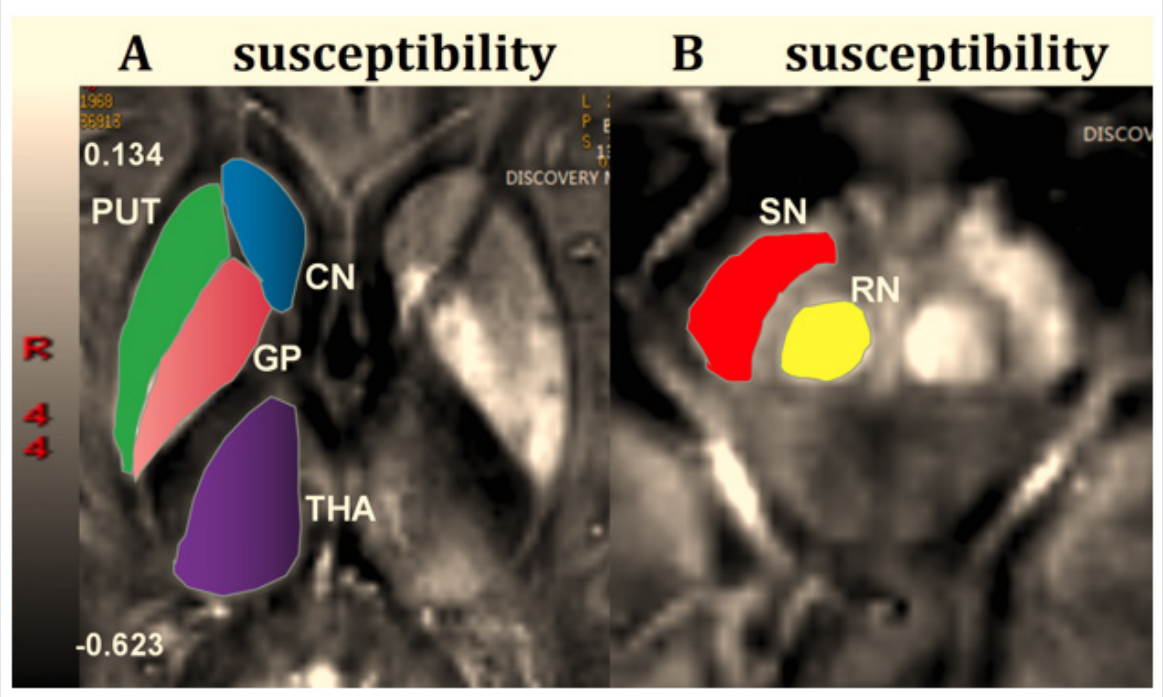

Figure 1:
A. Representative slice showing the ROIs for the CN, GP, PUT and THA.
B. The ROIs for the SN and RN. The ROIs were manually determined by the radiologic technologists.

Statistical Analysis

We used statistical software (StatView 5.0; SAS Institute, Cary, North Carolina). The results are expressed as the mean±SD. $p<0.05$ were considered statistically significant. Differences in the sex and age distribution were compared with chi-squared tests and t-tests. Because of the influence of age, differences in the magnetic susceptibility across the system of deep brain nuclei in the patients with PD (early and advanced stages) and controls were analyzed with ANCOVA. For pairwise multiple comparisons, the LSD (Least Significant Difference) was used. Multivariate analysis was performed to identify the best weighted combination of magnetic susceptibilities of all of these nuclei as a new biomarker for discriminating PD patients from controls, early-PD patients from controls and early-stage patients from advanced-stage patients with PD. To achieve this aim, a linear

discriminant analysis (LDA) method was used, and an LDA score was evaluated for differential diagnosis. To clarify the effectiveness of the various individual magnetic susceptibilities in these nuclei (CN, GP, PUT, THA, SN and RN) and a new imaging biomarker derived from LDA (LDA biomarker), ROC curves for the linear classifier were calculated, and the area under the curves (AUC) were evaluated. The correlations of the magnetic susceptibility among each region within these nuclei were analyzed by using Pearson's correlations (moderate correlation: 0.5≤R<0.8; mild correlation: 0.3≤R<0.5).

Results

Characterizing Iron Deposition in PD patients

Magnetic susceptibilities of all regions in the controls and PD patients were summarized in (Table 2 & Figure 2). Magnetic susceptibilities in these nuclei from the control group to the early PD group to the advanced PD group showed an increasing trend. Compared with controls, the PD patients had magnetic susceptibilities that were significantly increased in the THA and PUT but not in the SN, RN, CN or GP. Magnetic susceptibility of the THA was also significantly increased between controls and early-stage PD patients (p=0.037). However, the susceptibilities in all regions were not significantly different between the subgroups of PD patients.

Table 2: Comparison of magnetic susceptibility in deep nuclei between the PD and control groups (mean±SD).

Nuclei	Controls	Parkinson's disease			p value			
		Early stage	Progressive stage	Summary	Control vs. PD	Control vs. early stage	Control vs progressive stage	Early stage vs. progressive stage
CN	0.022 ±0.010	0.027 ±0.011	0.030±0.013	0.028±0.012	0.104	0.244	0.080	0.455
PUT	0.070 ±0.029	0.091 ±0.038	0.092 ±0.026	0.091±0.033	0.040	0.073	0.075	0.885
GP	0.109 ±0.038	0.125 ±0.040	0.130 ±0.028	0.127±0.035	0.102	0.188	0.117	0.696
THA	0.001 ±0.009	0.008 ±0.009	0.006 ±0.012	0.007±0.010	0.042	0.037	0.173	0.533
SN	0.067±0.031	0.068 ±0.020	0.077 ±0.019	0.071±0.020	0.524	0.912	0.253	0.266
RN	0.075 ±0.040	0.093 ±0.020	0.100 ±0.017	0.096±0.019	0.076	0.363	0.112	0.566

Note: Measuring disease progression in early Parkinson's disease: the National Institutes of Health Exploratory Trials in Parkinson's Disease (NET-PD) experience. The unit is ppm.

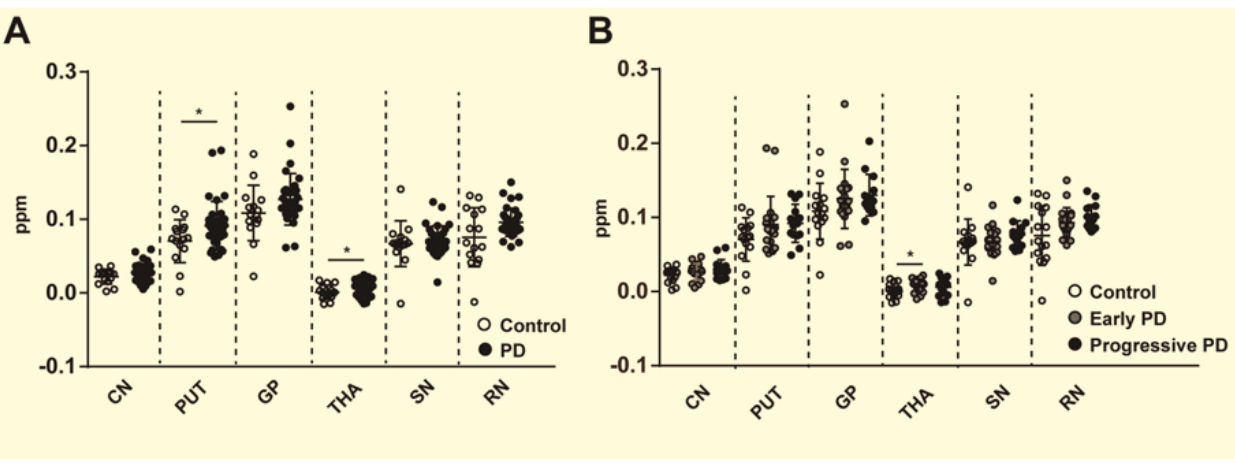

Figure 2:
A. ROI-based mean magnetic susceptibilities between the control and PD groups.
B. Comparison of the magnetic susceptibility of each ROI among controls and the two subgroups of PD patients. * p<0.05, **p<0.01.

Correlations Between Magnetic Susceptibility in Each Region

Figure 3 showed that there were some significant positive correlations among the magnetic susceptibilities of the CN, GP, PUT, THA, SN and RN. The magnetic susceptibility of the GP showed a significant moderate correlation with that of the PUT (R=0.575, P<0.01) and showed a significant mild positive correlation with that of the RN. A significant mild positive correlation was observed between magnetic susceptibility of the PUT and CN. In addition, the magnetic susceptibility of the RN displayed a moderate positive correlation with that of the SN (R=0.564, P<0.01). The magnetic susceptibility displayed mild or moderate positive correlations among the GP, PUT, SN and RN.

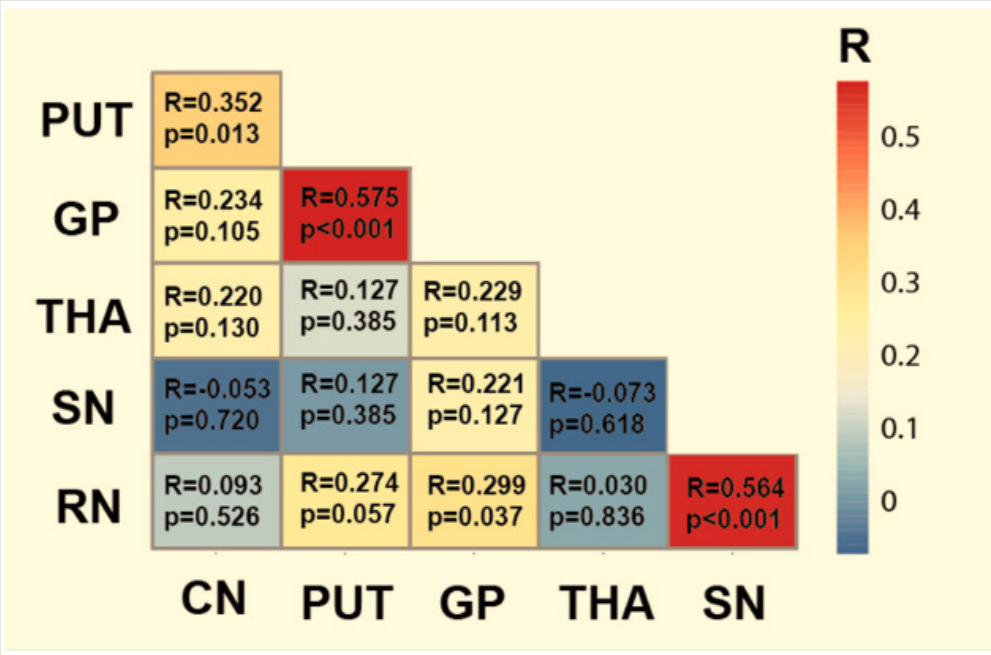

Figure 3: Heatmap showing the correction of magnetic susceptibility of each ROI within the basal ganglia system. Correlation coefficients and statistical significance are described in the graph. *p<0.05, **p<0.01.

ROC Curve Analysis of the Susceptibility of Each Region and the LDA Biomarker in PD Evaluation

Figure 4 displayed the magnetic susceptibility of each ROI and a new biomarker derived from LDA for PD diagnosis and evaluation. The LDA biomarker had the highest AUC (AUC=0.784, P=0.002) to distinguish PD patients from healthy controls, followed by the magnetic susceptibility of the THA and GP (Figure 4A). For the diagnosis of early-stage PD, the LDA biomarker had the highest AUC (AUC=0.777, p=0.006), which was followed by the magnetic susceptibility of the THA, GP and RN (Figure 4B). In addition, only the LDA biomarker had a notable discrimination ability in assessing the severity and progression of PD (AUC=0.714, p=0.036), followed by the magnetic susceptibility of the SN (Figure 4C). The magnetic susceptibility of the SN had the lowest AUC for classifying PD patients (0.549) and an early-stage PD diagnosis (0.510), and its AUC increased up to 0.632, following the LDA biomarker for the discrimination of PD subgroups. The LDA biomarker displayed the best diagnostic power, not only in PD identification but also in the earlystage diagnosis and assessment of PD. LDA score in each group was calculated for each patient by using a formula derived from the magnetic susceptibilities of these six regions within the deep nuclei weighted by their regression coefficient.

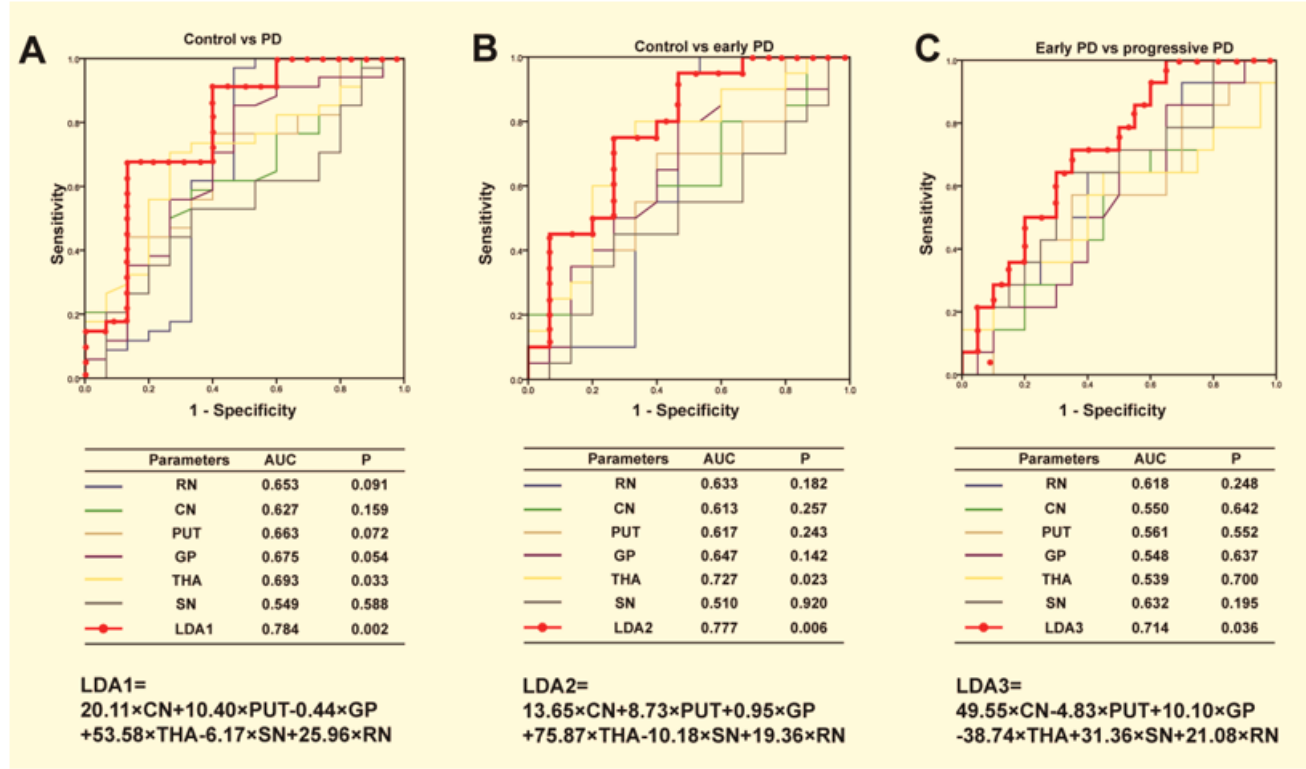

Figure 4: ROC curves for the magnetic susceptibility of the CN, GP, PUT, THA, SN, RN and LDA biomarker. AUC and statistical significance are described in the graph. AUC: area under the curve.

Discussion

Abnormal iron depositions were observed in the current study, and all magnetic susceptibilities of these nuclei (including the CN, GP, PUT, THA, SN and RN) showed heterogeneity increases in PD patients. By now, QSM is the most accurate and sensitive technique for iron quantification [8-10]. Our results confirmed previous results that magnetic susceptibilities increased inhomogeneity in all measured nuclei of PD patients compared to controls. The magnetic susceptibility of the GP was the highest, followed by that of the PUT and RN. Prior studies have reported that significantly increased iron in the SN and GP was a robust biomarker or, perhaps, the only valid indicator to identify PD patients and assess disease progression [6,11,15]. However, whether the increase in iron concentrations in the SN and GP contributes to PD has been controversial. Our results were consistent with some previous research results in that the iron deposition in the SN [7,13] and GP (6) did not show significant differences between the controls and PD patients. Uchida, et al. [13] demonstrated that the voxel-based analysis failed to show that the susceptibility of (parts of) the SN could predicted PD. Previous studies have revealed that regional changes were much sensitive than global changes, opening a promising door to separate high iron content patients from normal iron content patients [23-25]. Averaging over the whole nuclei based on traditional ROI-based approaches will reduce the chance of iron content differences, which resulted in a decrease in the diagnostic performance in detecting PD [18,24].

Furthermore, the sample sizes were limited, which may have impacted the statistical power. The magnetic susceptibility of the PUT and THA were both significantly increased in PD patients, and the susceptibility of the THA could readily distinguish early-onset PD patients from controls. Regarding the iron levels in the PUT of PD patients, these findings seem to be consistent with previous studies [18,25] that found that brain iron deposition in the PUT was of great value in distinguishing PD patients from controls. The PUT, as the main component of the striatum as well as the SN, is the major pathological change in PD. Brain iron does not readily cross the blood–brain barrier, which might suggest non-homogeneous iron transport from one structure to another in the brain, leading to abnormal deposition in certain functional regions in PD patients. Therefore, the accumulation of brain iron is not homogeneous in these deep nuclei in PD patients, as demonstrated in previous reports [23-25], and the results of the present study confirmed this characteristic. However, the mechanisms contributing to iron deposition in these regions have not been clarified. Our results demonstrated markedly increased iron levels in different regions with positive mild or moderate correlations among

these nuclei (e.g., the GP, PUT, SN, and RN), especially between the GP and PUT (R=0.575) and between the RN and SN (R=0.564), suggesting that possible functional or fibrous connections exist between these nuclei.

Previous studies have demonstrated that there were structural and functional connections among these nuclei [15,16,26]. The fasciculla nigrale (FN), as a mineralized structure that connects the GP to the SN, has been hypothesized to be involved in iron transport between the midbrain and the basal ganglia [26]. A novel gradient distribution pattern of iron deposition in the FN (the iron disposition gradually increased from the medial aspect of the GP to the anterior aspect of the SN) was found in PD patients and could represent underlying tract dysfunction. These results demonstrated that the magnetic susceptibility of the GP was highest and that the magnetic susceptibility of the SN significantly increased in the progressive PD group. Combined with previous results [15,26,27], we speculated that abnormal brain iron deposition might have started in the striatum and moved to the SN along the FN structure. Furthermore, the previously suggested cerebellar pathways also played an important role in compensating for basal ganglia system dysfunction in PD patients [15]. The RN and THA may provide another point of functional intersection between the striato cortical and cerebello thalamo cortical motor pathways.

Increased iron in the RN and THA may reveal structural changes related to cerebello thalamocortical compensation in PD, and iron binding capacities may be increased in these regions with higher metabolism. Moreover, the magnetic susceptibility of the THA as a unique biomarker increased significantly in the early stage of PD, and we hypothesized that THA was located in the central region among these functional connections and may have higher metabolic requirements. Based on the above characteristics and neurological theories, we proposed the hypothesis that integrating the characteristics of iron deposition in each nuclei would be more conducive to elucidating the role of abnormal cerebral iron deposition in PD, thereby revealing the pathogenesis of the disease and assessing the progression of PD. To achieve this, the LDA method was used to integrate susceptibility across the system of deep brain nuclei as a new biomarker (LDA biomarker).

These results demonstrated that the LDA biomarker had the highest AUC (AUC=0.784) to classify PD patients, followed by the magnetic susceptibility of the THA and GP. Regarding an early PD diagnosis, the highest AUC was for the LDA biomarker (AUC=0.777), followed by the magnetic susceptibility of the THA. In addition, only the LDA biomarker had a clear discrimination ability in assessing the severity and progression of PD (AUC=0.714). These results confirmed our hypothesis, and to the best of our knowledge, LDA biomarker is a new promising biomarker to advance the diagnosis and assessment of PD. Differential diagnosis between PD and atypical parkinsonism (AP), mainly progressive multiple system atrophy (MSA) and supranuclear palsy (PSP), remains challenging. Previous studies [28,29] demonstrated that QSM allows quantification of tissue iron content and could be a promising approach for differential diagnosis between PD and AP. The distribution characteristics of magnetic susceptibilities in various nuclei were different in PD, PSP and MSA. Mazzucchi, et al. [29] reported that the highest diagnostic accuracy for PSP was observed for the substantia nigra (STN), RN and medial part of the SN, whereas in MSA, iron accumulation in the PUT was significantly higher, following the patterns of pathological involvement that characterize the different diseases.

Our study has some limitations. It was a cross-sectional study, and a comprehensive, longitudinal study on brain iron deposition in PD patients needs to be performed. The ROIs were manually delineated, and the accuracy needs to be improved. At the same time, the ROI was set at a specific section, however, the susceptibility varies within each nuclei such that the mean across the nuclei ignore spatial variability that may improve classification. The study ignores this within-nuclei variation by taking the mean over the nuclei, which can not accurately and comprehensively measure the characteristics of iron deposition in various parts, which may have affected the results. The SN was not further separated into pars compacts and pars reticulata because of the rather low resolution of the clinical GRE data [30]. When dividing the patients into subgroups of PD according to H & Y stages, the UPDRS-III scores were not evaluated, which may have affected the results of the sensitivity, specificity, and accuracy of the magnetic susceptibility for PD evaluation. Some patients recruited in this study were taking antiparkinsonian medications, which may have influenced the evaluation of the clinical status of the PD patients and interacted with the speed and amount of iron deposition. DTI can provide an indirect measure of dopaminergic degeneration within the SN, but this technique was not applied in this study. Studies comparing the results of DTI and QSM may help to clarify the pathological changes and pathogenesis of PD patients.

Conclusion

QSM mapping successfully and quantitatively displayed abnormal iron deposition with heterogeneity across the deep nuclei in PD patients. Magnetic susceptibilities were significantly increased in the PUT, GP and THA but not in the SN. The magnetic susceptibility of the THA was a promising biomarker for discrimination early-stage PD patients from controls. The iron contents in different regions had mild or moderate positive correlations with each other (GP, PUT, SN, and RN), indicating that various nuclei have various functional connections and cascading changes in structure or functionality. LDA biomarker based on QSM is a promising tool for early diagnosis of PD.

Acknowledgment

We would like to thank all of the PD patients, their families, and the investigators who participated in this trial.

Funding

This study was supported by the Key Specialty Cultivation Project of Foshan (Fspy3-2015013) and Medical Scientific Research Foundation of Guangdong Province of China (A2021493).

Author Contributions

ZFX contributed to the conception or design of the work. JZX, YBJ, YJR, WXW, MYG, and HMH contributed to the acquisition, analysis, or interpretation of data for the work. JZX, ZFX contributed to drafting of the work or revising it critically for important intellectual content. All authors approved the final version of the manuscript.

Conflict of Interest

The authors declare no conflict of interest.

References

1. Abbas MM, Koh WP, Tan EK, Louis C S Tan (2018) Positive predictive value of different methods for identifying Parkinson's disease cases in an epidemiological study. Parkinsonism Relat Disord 54: 119-120.
2. Adler C, Beach T, Zhang N, A Atri (2020) Low diagnostic accuracy for an early clinical diagnosis of parkinson's disease. Parkinsonism & Related Disorders 79: 73-74.
3. Dusek P, Roos PM, Litwin T, Susanne A Schneider, Trond Peder Flaten, et al. (2015) The neurotoxicity of iron, copper and manganese in Parkinson's and Wilson's diseases. J Trace Elem Med Biol 31: 193-203.
4. Hare DJ, Double KL (2016) Iron and dopamine: a toxic couple. Brain 139: 1026-1035.
5. Guangwei Du, Tian Liu, Mechelle M, Lan Kong, Yi Wang, et al. (2015) Quantitative susceptibility mapping of the midbrain in Parkinson's disease. Movement Disorders 31(3): 317-324.
6. Ghassaban K, He N, Sethi SK, Huang P, Shengdi C, et al. (2019) Regional High Iron in the Substantia Nigra Differentiates Parkinson's Disease Patients from Healthy Controls. Front Aging Neurosci 11: 106.
7. Khashayar Dashtipour, Manju, Camellia Kani, Pejman Dalaie, Andre Obenaus, et al. (2015) Iron Accumulation Is Not Homogenous among Patients with Parkinson's Disease. Parkinsons Dis 2015: 324843.
8. Langkammer C, Pirpamer L, Seiler S, Andreas Deistung, Ferdinand Schweser, et al. (2016) Quantitative Susceptibility Mapping in Parkinson's Disease. PLoS One 11(9): e0162460.
9. de Rochefort L, Liu T, Kressler B, Jing Liu, Pascal Spincemaille, et al. (2010) Quantitative susceptibility map reconstruction from MR phase data using bayesian regularization: validation and application to brain imaging. Magn Reson Med 63(1): 194-206.
10. Schweser F, Sommer K, Deistung A, Jürgen Rainer Reichenbach (2012) Quantitative susceptibility mapping for investigating subtle susceptibility variations in the human brain. Neuroimage 62: 20832100.
11. Murakami Y, Kakeda S, Watanabe K, I Ueda, A Ogasawara, et al. (2015) Usefulness of quantitative susceptibility mapping for the diagnosis of Parkinson disease. AJNR Am J Neuroradiol 36(6): 1102-1118.
12. An H, Zeng X, Niu T, Gaiying Li, Jie Yang, et al. (2018) Quantifying iron deposition within the substantia nigra of Parkinson's disease by quantitative susceptibility mapping. J Neurol Sci 386: 4652.
13. Uchida Y, Kan H, Sakurai K, Nobuyuki Arai, Daisuke Kato, et al. (2019) Voxel-based quantitative susceptibility mapping in Parkinson's disease with mild cognitive impairment. Movement Disorders 2019(2): 1164-1173.
14. Shibata H, Uchida Y, Inui S, Hirohito Kan, Keita Sakurai, et al. (2022) Machine learning trained with quantitative susceptibility mapping to detect mild cognitive impairment in Parkinson's disease. Parkinsonism & Related Disorders 94: 104-110.
15. Lewis MM, Du G, Sen S, A Kawaguchi, Y Truong, et al. (2011) Differential involvement of striato- and cerebello-thalamo-cortical pathways in tremor- and akinetic/rigid-predominant Parkinson's disease. Neuroscience 177: 230-239.
16. Du G, Lewis MM, Sica C, Lu He, James R Connor, et al. (2018) Distinct progression pattern of susceptibility MRI in the substantia nigra of Parkinson's patients. Mov Disord 33: 1423-1431.
17. Hwang EJ, Ryu DW, Lee JE, SH Park, HS Choi, et al. (2019) Magnetic resonance imaging assessment of the substrate for hyposmia in patients with Parkinson's disease. Clin Radiol 74(6): 489.e9-489.e15.
18. Zhang Y, Yang M, Wang F, Yiting Chen, Rong Liu, et al. (2022) Histogram Analysis of Quantitative Susceptibility Mapping for the Diagnosis of Parkinson's Disease. Academic Radiology 29(3): S71-S79.
19. Riffenburgh R H, Clunies Ross C W (2013) Linear Discriminant Analysis. Chicago 3(6): 27-33.
20. Su M, Chuang K S (2015) Dynamic feature selection for detecting Parkinson's disease through voice signal[C]// IEEE Mtt-s International Microwave Workshop Series on Rf & Wireless Technologies for Biomedical & Healthcare Applications. IEEE.
21. Chiu M J (2020) Classifications of Neurodegenerative Disorders Using a Multiplex Blood Biomarkers-Based Machine Learning Model Int J Mol Sci 21(18): 6914.
22. Adeli E, Shi F, An L, Chong Yaw Wee, Guorong Wu, et al. (2016) Joint feature-sample selection and robust diagnosis of Parkinson's disease from MRI data. NeuroImage 2016(141): 206-219.
23. He N, Ling H, Ding B, Juan Huang, Yong Zhang, et al. (2015) Region-specific disturbed iron distribution in early idiopathic Parkinson's disease measured by quantitative susceptibility mapping. Hum Brain Mapp 36(11): 4407-4420.
24. Ide S, Kakeda S, Ueda I, Keita Watanabe, Yu Murakami, et al. (2015) Internal structures of the globus pallidus in patients with Parkinson's disease: evaluation with quantitative susceptibility mapping (QSM). Eur Radiol 25(3): 710-718.
25. Guan X, Xuan M, Gu Q, Peiyu Huang, Chunlei Liu, et al. (2017) Regionally progressive accumulation of iron in Parkinson's disease as measured by quantitative susceptibility mapping. NMR Biomed 30(4).
26. Chen Q, Chen Y, Zhang Y, Furu Wang, Hongchang Yu, et al. (2019) Iron deposition in Parkinson's disease by quantitative susceptibility mapping. BMC Neurosci 20(1): 23.
27. Alahmadi A, Pardini M, Samson R, Egidio DAngelo, Karl J Friston, et al. (2015) Differential involvement of cortical and cerebellar areas using dominant and nondominant hands: An FMRI study. Human Brain Mapping 23(12): 5079-5100.
28. Peckham ME, Dashtipour K, Holshouser BA, Camellia Kani, Alex Boscanin, et al. (2016) Novel Pattern of Iron Deposition in the Fascicula Nigrale in Patients with Parkinson's Disease: A Pilot Study. Radiol Res Pract 2016: 9305018.
29. Mazzucchi S, Frosini D, Costagli M, Eleonora Del Prete, Graziella Donatelli, et al. (2019) Quantitative susceptibilitymapping in atypical Parkinsonisms. Neuroimage Clin 24: 101999.

30. Ito K, Ohtsuka C, Yoshioka K, Hiroyuki Kameda, Suguru Yokosawa, et al. (2017) Differential diagnosis of parkinsonism by a combined use of diffusion kurtosis imaging and quantitative susceptibility mapping. Neuroradiology 59(8): 759-769.

ISSN: 2574-1241

DOI: 10.26717/BJSTR.2024.55.008740

Zhi Feng Xu. Biomed J Sci & Tech Res

Submission Link: https://biomedres.us/submit-manuscript.php